



Issue №7

Part 1



International periodic scientific journal

ONLINE

www.sworldjournal.com

Indexed in
INDEXCOPERNICUS
(ICV: 69.6)

SWorld Journal

Issue №7

Part 1

March 2021

With the support of:

D.A.Tsenov Academy of Economics - Svishtov (Bulgaria)
Institute of Sea Economy and Entrepreneurship
Moscow State University of Railway Engineering (MIIT)
Ukrainian National Academy of Railway Transport
State Research and Development Institute of the Merchant Marine of Ukraine (UkrNIIMF)
Kharkiv Medical Academy of Postgraduate Education
Alecu Russo State University of Bălți
GUUPO "Belarusian-Russian University"
Institute of Water Problems and Land Reclamation of the National Academy of Agrarian Sciences
Odessa Research Institute of Communications

Published by:

SWorld & D.A. Tsenov Academy of Economics – Svishtov, Bulgaria

Editor: Shibaev Alexander Grigoryevich, *Doctor of Technical Sciences, Professor, Academician*
Scientific Secretary: Kuprienko Sergey, *PhD in Technical Sciences*

Editorial board: More than 200 doctors of science. Full list on pages 3-4

The International Scientific Periodical Journal "*SWorldJournal*" has been published since 2019 and has gained considerable recognition among domestic and foreign researchers and scholars.

Periodicity of publication: Quarterly

The journal activity is driven by the following objectives:

- Broadcasting young researchers and scholars outcomes to wide scientific audience
- Fostering knowledge exchange in scientific community
- Promotion of the unification in scientific approach
- Creation of basis for innovation and new scientific approaches as well as discoveries in unknown domains

The journal purposefully acquaints the reader with the original research of authors in various fields of science, the best examples of scientific journalism.

Publications of the journal are intended for a wide readership - all those who love science. The materials published in the journal reflect current problems and affect the interests of the entire public.



UDC 620.22

STRUCTURAL PHASE PROCESSES IN MULTICOMPONENT METAL CERAMIC OXIDE MATERIALS BASED ON THE SYSTEM Y–Ti–Zr–O (Y₂O₃–TiO₂–ZrO₂)

СТРУКТУРНО-ФАЗОВЫЕ ПРОЦЕССЫ В МНОГОКОМПОНЕНТНЫХ МЕТАЛЛОКЕРАМИЧЕСКИХ ОКСИДНЫХ МАТЕРИАЛАХ НА ОСНОВЕ СИСТЕМЫ Y–Ti–Zr–O (Y₂O₃–TiO₂–ZrO₂)

Chyshkala V. O. / Чишкала В. А.

d.t.s., as.prof. / к.т.н., доц.

ORCID: 0000-0002-8634-4212

Lytovchenko S. V. / Литовченко С. В.

d.t.s., prof. / д.т.н., проф.

ORCID: 0000-0002-3292-5468

V. N. Karazin Kharkiv National University, Kharkiv, Svobody sq., 4, 61022

Харьковский национальный университет имени В. Н. Каразина,

Харьков, пл. Свободы 4, 61022

Gevorkyan E. S. / Геворкян Э. С.

d.t.s., prof. / д.т.н., проф.

ORCID: 0000-0003-0521-3577

Nerubatskyi V. P. / Нерубацкий В. П.

d.t.s., as.prof. / к.т.н., доц.

ORCID: 0000-0002-4309-601X

SPIN: 5106-4483

Morozova O. M. / Морозова О. Н.

postgraduate / аспирантка

ORCID: 0000-0001-7397-2861

Ukrainian State University of Railway Transport, Kharkiv, Feiervakh sq., 7, 61050

Украинский государственный университет железнодорожного транспорта,

Харьков, пл. Фейербаха, 7, 61050

Abstract. The article investigates the synthesis processes, structural characteristics and structural-phase processes in multicomponent metal-ceramic oxide materials based on the Y-Ti-Zr-O system (Y₂O₃-TiO₂-ZrO₂), synthesis of ultra- and nanodisperse oxide powders of the Y-Ti-Zr-system. O, development and improvement of methods of compaction and consolidation of materials based on them, determination of structural characteristics of oxide materials and the impact of technological processes on these characteristics. The structural-phase evolution in the production of yttrium and titanium oxides, as well as compact ceramics based on them with the structure of pyrochlorine has been studied. Samples of oxide powders were obtained and compact and consolidated ceramics with different content of pyrochlorine phase of Y₂Ti₂O₇ oxides were made, high-temperature influence technology was optimized to increase the content of this phase in ceramic samples. It is recorded that the increase in the term of high-temperature exposure leads to an increase in the content of the pyrochlorine phase.

Key words: multicomponent composites, DZO-steels, alumina, titanium oxide, ultra- and nanodisperse powders, consolidated materials, ceramics, compaction.

Introduction.

Recently, nanotechnology and nanomaterials have become an interdisciplinary field of science and technology. In their development, these areas could not but affect the development of the nuclear sphere: nuclear technology, nuclear energy, nuclear materials [1].



Further economically justified, socially attractive and technologically safe use of nuclear energy, development of nuclear energy, nuclear industry and nuclear technologies are impossible without modernization of known and creation of new fuels and construction materials of nuclear reactor core. One of the possible ways to improve or create new nuclear materials is the use of nanotechnology, which has recently been increasingly used in almost all areas of new technologies [2, 3].

Providing new properties of fuel and structural materials of the nuclear industry is possible with the use of nanotechnology in the transition in materials to the nanometric range of sizes. Areas of implementation of nanotechnology in nuclear energy today are almost the entire nuclear fuel cycle, including the creation of new nuclear fuel with nanoadditives, the creation of nanodispersed materials for structural and functional purposes (dispersion-oxide-reinforced ferritic martensitic steels, so-called SDC steels). to name researches of radiation-induced structure of materials, nanomembranes and nanofilters for technologies of management of radioactive waste, nanosensors and sensors for control systems and other [4, 5].

The most promising direction in the development of materials for nuclear power devices of the next generations is the creation of new materials based on ferritic-martensitic radiation-resistant steels. Such new materials are the so-called DZO-steels – alloys, the steel matrix of which is strengthened by oxide particles (simple or complex) of nanometer size. The development of such materials is now a world-class problem, involving large groups of scientists from many countries. An additional incentive to these studies are the unique characteristics of SDC steels (mechanical properties, radiation resistance, high temperature stability), which allow us to plan the use of such materials in thermonuclear devices.

The above problems of scientific and technological development emphasize the relevance and importance of developing technologies for creating bulk ultra- and fine crystalline materials and fine powders of metals, alloys and compounds intended for use in various fields of science, technology and production, as the special properties of these materials can provide new operational characteristics of products from them [6, 7]. Three-dimensional (massive) ultra- or nano-grained materials are made either directly from solid crystalline or amorphous materials, or by methods of powder technology (production of dispersed powder materials and subsequent operations of their compaction and consolidation). It is determined (primarily on metals) that reducing the size of structural elements (particles, crystallites, subgrains) below a certain limit value can lead to a noticeable change in properties.

Changing the particle size in materials can cause a significant change in its properties. Such changes are often called "dimensional effects". This term covers a wide range of phenomena related to changes in the energy state of the system and its thermodynamic characteristics, including the contribution of particle distribution boundaries to the properties of the whole system, as well as compatibility of particle size with physical parameters having length dimension. These and a number of other features of the structure of nanocrystalline materials determine the properties of such materials, which differ significantly from conventional polycrystals. Based on this, reducing the grain size may be a possible or potentially effective method of changing the properties of the solid. When studying the properties of ultrafine structural



materials, it is necessary to take into account not only their composition and structure, but also the dispersion and size distribution of particles. Polycrystalline materials with an average grain size of 300 to 40 nm are usually called submicrocrystalline, and with an average grain size less than 40 nm – nanocrystalline.

An important feature of nanomaterials, which significantly affects the stability of their structure and corresponding properties, is the extremely high mobility of atoms, which causes active diffusion by grain boundaries. Quantitative indicators of such mobility in $10^5 \dots 10^6$ are greater than similar characteristics of conventional polycrystals, although today there are significant differences in understanding the mechanisms of diffusion processes in nanocrystalline substances, available in the literature on this information and explanations are often the same.

The nanocrystalline state of matter is one of its possible nonequilibrium metastable states. Its difference in comparison with other known non-equilibrium states of matter is the lack of an equilibrium state, which corresponds to it in three-dimensional and two-dimensional structures (bulk elements – crystallites and surface elements – development, plane of boundaries).

Nanocrystalline materials are a special state of condensed matter – macroscopic ensembles of ultra-small particles up to several nanometers in size. Unusual properties of these materials are due to the characteristics of individual particles (crystallites) and their collective behavior, and also depend on the nature of the interaction between nanoparticles [8].

Physico-mechanical properties of materials created by powder technologies depend on a number of characteristics, including the composition (both chemical and mineralogical), structural parameters of the original ingredients (dispersion of particles, their shape, particle size distribution, size distribution, etc.), the value of the surface energy of particles of different size and composition.

Among ternary metal oxides, compounds with the generalized formula $A_2B_2O_7$ (where A and B are metals), a family of oxides with the same phase structure of mineral pyrochlor (NaCa) (NbTa) $O_6F / (OH)$ can be separated into a separate group [9].

The spatial group of an ideal pyrochlorine structure is $Fd(-3)m$ with eight molecules in a unit cell ($Z = 8$). In pyrochlores of the general formula $A_2B_2O_7$, element A is usually a trivalent rare earth metal, but in some cases it may be another mono- or divalent cation. Element B can be transition $3d$, $4d$ or $5d$ metals in the appropriate oxidation state to form the desired composition [10]. The structure of pyrochlores is close to fluorite (compounds of type AX_2), the difference is that in pyrochlores there are 2 cationic nodes, and from one to eight anions are absent (Fig. 1, 2).

For ordered pyrochlor with a composition corresponding to stoichiometry ($A_2B_2O_7$), the phase stability of the structure is mainly determined by the ratio of the radii of atoms A and B. Moreover, in the case of close radii, the formation of a disordered structure of fluorite is more likely than ordered pyrochlor. For example, the compound $Er_2Zr_2O_7$ with a radius ratio $r_A/r_B \sim 1.39$ has the structure of disordered fluorite, and the compound $Er_2Ti_2O_7$ with a ratio $r_A/r_B \sim 1.66$ is ordered pyrochlor.

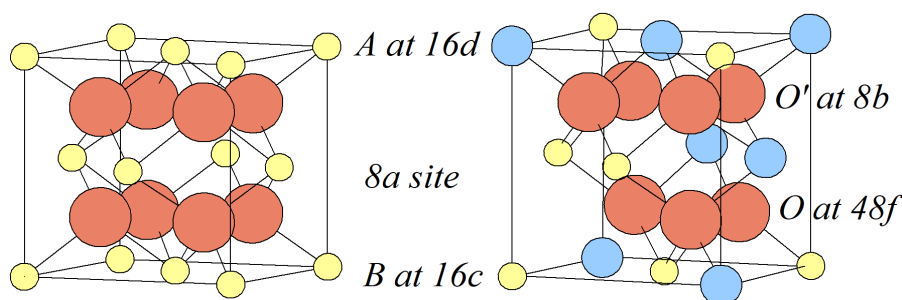
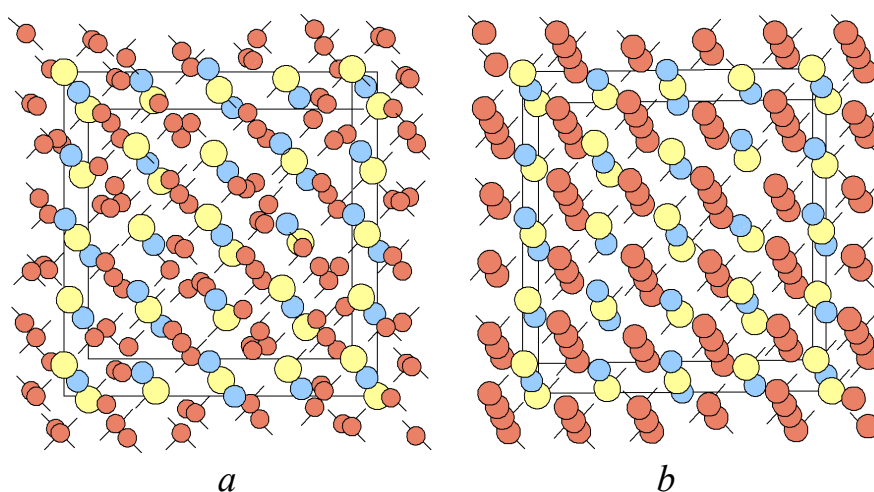


Fig. 1. On the left - an elementary cell of fluorite (Fmm), small atoms – cations A^{4+} ; large atoms – O_2 anions; on the right – 1/8 of the unit cell of pyrochlore (Fdm), small atoms – cations B^{4+} , medium atoms - cations – A^{3+} , large atoms – anions O_2



**Fig. 2. Pyrochlorine structure (complete unit cell):
a – reflection of weakened positions $Gd_2Sn_2O_7$ ($X = 0.3348$);
b – reflection of idealized fluorite positions ($X = 0.375$)**

Today, researchers focus not only on pyrochlores with cations (3+, 4+), but also on compounds with other cationic indicators of elements, in particular (2+, 5+), (1+, 6+), for example, KOs_2O_6) [11]. A feature of pyrochlores is a significant and wide variation of physical properties depending on the elemental composition and structural-phase state. So, the electrical properties of pyrochlores vary from insulators and semiconductors to metallic conductivity. A number of pyrochlores with the composition REM–Mo and REM–Ru demonstrate the transition of metal-semiconductor properties. Pyrochlore of $Cd_2Re_2O_7$ is a superconductor at low temperatures [12, 13].

Systems where ions A and B are in a state of maximum oxidation, exhibit dielectric properties. The electrical properties of bismuth-containing pyrochlores (for example, $Bi_2Ru_2O_7$) are determined by the pair of free electrons of bismuth. $La_2Zr_2O_7$ pyrochlores are used to create a thermal barrier, and $Y_2Sn_2O_7$ pyrochlores are an acceptable material for making matrices of photoluminescent devices. Some pyrochlores, when properly selected, can be oxide electrolytes with ionic conductivity [14, 15].

An important property of pyrochlores is their sensitivity to pressure. Thus, under the action of high pressure pyrochlores can go into the fluorite phase, and sometimes



even go into a state of a mixture of substances that were the source in the formation of pyrochlore (mixture of oxides) [16, 17].

It should be noted that pyrochlores can act as a matrix material for immobilization of radioactive waste. It was found that the stability of pyrochlores under the influence of irradiation increases with decreasing ratio of the radii of atoms of its cations, which can be explained by the formation of certain defects in its structure. The energy accumulated by the substance as a result of irradiation can be dissipated by mutual permutation of cations A and B, and in this case the structure of pyrochlore is converted into defective fluorite. However, in the case when pyrochlores have a large difference in the ionic radii of the cations, this change in the positions of the ions becomes impossible. Because of this, at high radiation doses, such pyrochlores are amorphized. Such a restructuring is necessary to dissipate additional energy. An example of a material with the described properties is the compound $\text{Gd}_2\text{Zr}_2\text{O}_7$, such material was selected as a carrier material for the fixation of some nuclear waste [18, 19].

Recently, work on the creation and study of electrical and radiation properties of pyrochlores, in particular the creation of four-component compounds (for example, $\text{Y}_2\text{Zr}_{1.2}\text{Ti}_{0.8}\text{O}_7$), the manufacture of pyrochloride solid electrolytes for hydrogen fuel cells, and the formation of pyrochlores. The latter can be used in the development of radiation-resistant steels dispersed by oxide nanoinclusions, the so-called SDC steels.

The work continues the research performed by the authors in previous years, and is based on the results and scientific achievements, partially published in the works [20–23].

Main text.

Currently, two schemes for obtaining materials with pyrochlore structure have been developed and are used. This is, firstly, the sintering of oxide powders and, secondly, sol-gel technology. For each elemental composition of the substance has its own temperature range of the pyrochlorine phase.

The sol-gel method is a fairly common method of obtaining various ceramic nanomaterials, including oxide compounds [24]. A mandatory component of sol-gel technology is the formation of a colloidal solution in which elements can coexist that cannot coexist in ordinary solutions. The process of deposition from colloidal solutions belongs to a number of methods that involve the technological operation of dissolving components. The standard sol-gel method is a sequential set of certain operations, in particular, we can distinguish: preparation of a solution of the precursor (starting component – reagent or substance involved in intermediate reactions in the synthesis of the final product), transfer of this solution into sol (two-phase system formed by colloidal particles distributed in the liquid), the subsequent implementation of the processes of hydrolysis and condensation to convert the sol into a gel (interconnected solid three-dimensional grid with submicron pores that are filled with liquid or gas). Then there may be stages of aging of the gel, its heat or other treatment. Usually the final stage is annealing or calcination.

One of the most important advantages of the method is the possibility of wide variation of the ratio of components. The specific mechanical properties of sols and gels create the preconditions for the manufacture of this technology not only nano-



and ultrafine powders (objects of zero-dimensional geometry), but also fibers (one-dimensional), films (two-dimensional) and bulk composites (three-dimensional volumes). The most commonly used variants of the method are technologies based on different variants of mixing the source components or removing the solvent.

Methods of chemical precipitation consist in the joint precipitation (coprecipitation) of product components from solution in the form of insoluble salts or hydroxides. The most common are three variants of chemical precipitation – hydroxide, oxalate and carbonate methods.

This method produces powders with a grain size of at least one hundred nanometers. Obtaining smaller particles is complicated by the fact that the finishing process is high-temperature processing (annealing) of the precursor at a temperature of about 1,000 °C (and even higher temperatures), during which there is a high probability of sintering and active agglomeration of particles.

The usual method of obtaining nanoparticles from colloidal solutions is to implement a chemical reaction between the components of the solution and the planned interruption of this reaction at a certain point in time, after which the dispersed system goes from a liquid colloidal state to a dispersed solid.

The growth of nanoparticles is interrupted, for example, by an abrupt increase in the hydrogen index (pH) of the solution. It is much easier to obtain colloidal particles of metal oxides by hydrolysis of salts. Nanocrystalline oxides of titanium, zirconium, yttrium can be obtained by hydrolysis of the corresponding chlorides or hypochlorides, followed by calcination of the amorphous precipitate at temperatures of 700...1,000 °C.

The formation of a jelly-like gel can be initiated by different variants, each of which leads to the formation of a different structure (so-called micellar or polymeric structure).

The results of our previous research and analysis of known data necessitated additional study of the synthesis of individual oxides (yttrium oxide, titanium oxide), the implementation of technologies to influence their structural state to form the desired crystalline forms and study the influence of external factors on the evolution of structural phase multi-element oxides.

The main direction of the experimental work was to study the process of synthesis of multielement oxide compounds of Y–Ti–Zr–O (Y_2O_3 – TiO_2 – ZrO_2), in particular yttrium and titanium oxides, to determine the influence of technological factors on the structural and phase state of materials and some of their mechanical properties.

A number of methods for the synthesis of ultra- and nanodisperse powders of both individual (single-phase) oxides and complex oxides of the Y–Ti–Zr–O system were mastered and the possibility and acceptability of their use for the formation of substances of a certain composition and structure were determined. Adaptation of methods of compaction and consolidation of oxide materials is performed and samples of metal-ceramic materials for research of properties are received.

To obtain oxide powders, methods of chemical dissolution and thermal decomposition of salts were used, followed by evaporation of water and special heat treatment.



The thermal effect on the samples is realized in chamber-type air furnaces, which are structurally similar, but differ in geometric dimensions and maximum operating temperature. The large chamber furnace consists of a heating chamber measuring $40 \times 30 \times 20 \text{ cm}^3$, which is housed in a metal housing. The heat-insulating lining of the chamber is made of porous ceramics, the surface of which is strengthened by special chemical treatment. Heating elements are fixed on the side walls of the chamber. Heaters made of fechril (brand X23U5T) wire with a diameter of 2 mm are made in the form of spirals and placed in protective ceramic tubes. The heating chamber is closed by a door, which is fixed by a suitable device.

The small chamber furnace has a cylindrical working chamber with a diameter of 100 mm and a height of 150 mm, its spiral heaters were made of nichrome wire with a diameter of 1.4 mm brand X20N80.

Power supply of furnaces is provided by the special electronic blocks which are intended for regulation of necessary power, and also for software control of a temperature mode of furnaces. At temperatures up to $1,200^\circ\text{C}$, the temperature sensor is a thermocouple HA (chromel-alumel), and at higher temperatures - a thermocouple TsNIICHM-1 (tungsten and an alloy of molybdenum with aluminum). Electronic units have indicators of input power (voltage and input current of each phase). Designs provide protective shutdown of power supply at opening of doors of furnaces. The rate of heating of furnaces to the set temperature is regulated by the established indicator of the maximum power. In the case of individual experiments, the heating rate was 5°C per minute. Temperature fluctuations in the working chambers of the furnaces during high-temperature exposure of the samples did not exceed $\pm 10^\circ$.

Metallographic characteristics of manufactured ceramic samples and the evolution of the structure due to external influences were determined by optical microscopy (MIM-8, Metam P-1). Eyepiece webcams (USB-300 and Levenhuk C 130NG) were used to capture images of metallographic structures. When performing optical microscopy (OM), light field illumination was used to form images and analyze the macro- and microstructure of materials. Samples for research were sections, which were prepared according to standard methods.

Phase analysis of the synthesized materials was determined by sciagrams diffractometry (DRON-3M and DRON-4-07).

Diffractograms were obtained in cobalt $\text{Co-K}\alpha$ (wavelength $\lambda = 0.179026 \text{ \AA}$) and copper $\text{Cu-K}\alpha$ (wavelength $\lambda = 1.5418 \text{ \AA}$) radiation using an iron or nickel selective absorbing filter under Bragg-Brentano focusing conditions. Sciagrams scanning of the surface of the samples in the range of angles 2θ from 10° to $90 \dots 100^\circ$. After diffraction of sciagrams on the samples, its registration was carried out with a scintillation detector.

Qualitative sciagram phase analysis consisted in comparing the spectra obtained from the studied samples with the diffraction spectra of the standards - pure phases, the presence of which is probable in the samples. Based on the results of this comparison, a simple list of detected substances or compounds was formed. Qualitative phase analysis was performed according to the file of the international



database ICDD PDF-2.

The content of the phases was quantified on the assumption that the intensity of the lines of a certain phase is proportional (including) to the volume fraction of this phase in a complex composition. This approach does not allow to determine the content of the phases in the composition with due accuracy, but may be acceptable for comparison with one or another accuracy of the content of one phase relative to another.

Rietveld's method was used for more accurate quantitative phase analysis of samples and determination of crystal lattice parameters of existing phases.

An IR-29 spectrophotometer (LOMO) was used to record the absorption spectra in the IR range. The spectra were recorded in the range of $4,000...400\text{ cm}^{-1}$ (middle infrared region). The powders obtained by grinding the sintered samples in agate mortars to a particle size of $\sim 1...10\text{ }\mu\text{m}$ were investigated. Samples were prepared in the form of clear compressed tablets from a mixture of KBr, which served as a matrix, and the test substance (1 %, sample 100 mg). The tablets were rectangular in shape and $25\times 5\text{ mm}$ in size. The pressing pressure was $9,200\text{ kg/cm}^2$. To exclude the absorption bands of the matrix in the comparison channel of the device contained a tablet of pure potassium bromide, which was pre-dried at $180\text{ }^{\circ}\text{C}$ for 10 hours. Pressing was performed immediately before the registration of the spectra. Graduation was performed on the spectrum of polystyrene with known frequencies of absorption maxima. The average value of the correction was $5...10\text{ cm}^{-1}$.

At the first stage of the work they tried to adapt the technology of obtaining yttrium oxide by thermal decomposition of nitrate salt $\text{Y}(\text{NO}_3)_3$ on the existing technological equipment. An ingot of fused yttrium brand ITM-1 weighing about 30 g was completely dissolved in 20 % nitric acid solution, taken in excess (based on the yield of the chemical reaction). After dissolution, the liquid was filtered (4 steps) to remove undissolved impurities and mechanical contaminants. After the final filtration, the liquid visually looked completely transparent, no foreign particles were observed.

The resulting solution was divided into portions (capacity $\sim 50\text{ ml}$), poured into flat porcelain crucibles and subjected to evaporation at different temperatures (series A at $T_1 \sim 130\text{ }^{\circ}\text{C}$, series B at $T_2 \sim 520...580\text{ }^{\circ}\text{C}$, series C at $T_3 \sim 240\text{ }^{\circ}\text{C}$). Air furnaces with a temperature field homogenizer (purified sand) were used to heat the liquid. The temperature was measured by thermocouple method on the outer surface of the porcelain crucible. The duration of evaporation ranged from 1 to 5 hours.

After evaporation in all experiments received ultrafine white powder. The resulting white precipitate was placed in an air furnace and calcined at different temperatures: samples of series A according to the first variant (one-stage heat treatment) – heating to $800\text{ }^{\circ}\text{C}$ ($1...1.5\text{ hours}$), endurance – 0.5 hours; samples of series B and C according to the second option (two-stage heat treatment) – first (stage 1) heating to $400\text{ }^{\circ}\text{C}$ ($0.5...1\text{ hour}$), exposure at this temperature – 3 hours; then (stage 2) – raising the temperature to $920\text{ }^{\circ}\text{C}$ (1.5 hours), the second exposure – 10 hours.

After heat treatment, sciagram diffractometric analysis of the samples was performed (Fig. 3).

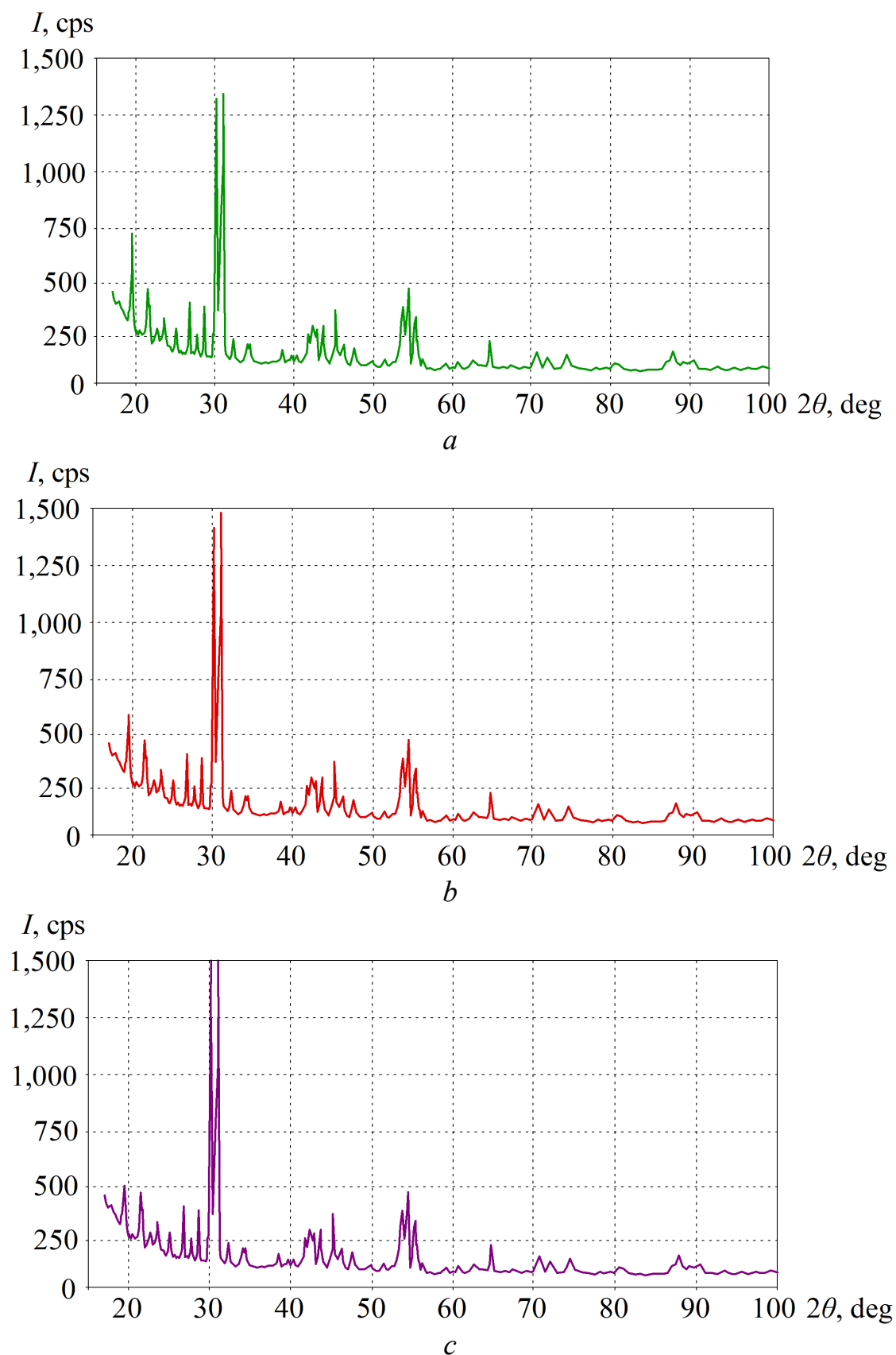


Fig. 3. Radiographs of samples of series A (a), B (b) and C (c), respectively, after heat treatment

All obtained radiographs are identical within the statistical error. The desired Y_2O_3 phase and the initial $\text{Y}(\text{NO}_3)_3$ phase have not been identified. The most



probable phase for sciagram peaks is substance $Y_2(SO_4)_3$, the reliability of identification is about 70 %. Note that under the conditions of the experiment, the formation of such a substance is impossible. Analysis of the obtained data leads to the assumption that the obtained powder material is a complex compound (mixture of compounds) type $Y_4O(NO_3)_{10}$, $Y_4O_2(NO_3)_8$, $Y_4O_4(NO_3)_4$ or $Y_4O_5(NO_3)_2$. The next stage of the work was devoted to the study of the realization of the possibility of synthesis of pyrochlores of the $Y_2Ti_2O_7$ type, which are similar to the compound $Y_2Zr_2O_7$.

The properties of materials with pyrochlore structure can vary within wide limits when using different types of processing. This effect can vary the crystal structure, coefficient of thermal expansion, conductivity, sintering and other characteristics. In particular, the pyrochloride compound $Y_2Ti_2O_7$ after annealing and sintering at 1,550 °C for 12 hours increases its electrical conductivity by two orders of magnitude, which can be explained by the formation of the $YTiO_{2,085}$ phase with a noticeable oxygen deficiency compared to the original compound due to transformation of Ti^{4+} to Ti^{3+} at low oxygen.

The technology proposed in [25] is quite energy-intensive, as it is based on long-term processing at fairly high temperatures. It is desirable to adapt the technology to lower temperatures.

The starting ingredients were powders of yttrium oxides Y_2O_3 and titanium TiO_2 of industrial production.

Under normal conditions, yttrium oxide has a cubic lattice, polymorphic transformations are possible either at very high temperatures (at 2,277 °C the transformation of the lattice from cubic to hexagonal syngony), or at elevated pressure (at a pressure of 3.5 MPa and a temperature of 550 °C monoclinic syngony). As it was planned to use technological operations within the existence of the cubic phase of yttrium oxide, no additional initial processing of this powder was carried out.

Titanium oxide crystallizes in cubic syngony (rutile), rhombic syngony (brookite), tetragonal syngony (anatase), as well as possible rhombic IV and hexagonal V modifications.

Rutile, brookite and anatase can exist under normal conditions and at elevated temperatures, therefore to ensure the use of cubic phase TiO_2 in the synthesis of pyrochlore, additional heat treatment of the initial titanium oxide powder was applied to ensure the formation of rutile.

Since yttrium oxide powder also had to be stripped of adsorbed water and gases, primarily CO_2 , its heat treatment was carried out simultaneously with the heat treatment of yttrium oxide powder in separate crucibles. Annealing was carried out in an air furnace at temperatures of 750...1,000 °C for 0.5...4 hours, which was sufficient for the distillation of absorbed gases and water vapor, as well as the flow of structural changes in titanium oxide. According to the research results, the temperature of 850 °C and the duration of exposure at this temperature of 1.5 hours can be recommended as optimal annealing conditions. After turning off the furnace heater, the door was not opened and the powders were cooled together with the furnace to a temperature of 200...300 °C, then taken out into the air and mixed in a



ratio of 1:1 (atomic percent), which corresponds to 58.6 % Y_2O_3 and 41.4 % TiO_2 .

For the manufacture of samples took: Y_2O_3 – 12.54 g; TiO_2 – 8.87 g. Accuracy of weight determination ± 0.01 g.

The mixture of powders was stirred in a porcelain mortar for 1 hour. The main (about 50 %) fraction of powders was a fraction with a particle size of 1...2 μm . There are also smaller (nanoscale) particles and their agglomerates, and a fraction of up to 5 μm (up to 15 %), as well as a small (several percent) fraction of larger particles.

The resulting mixture was divided into separate portions, which made a series of compacts of 6 samples. Compaction of powder mixtures by pressing was performed in a steel cylindrical mold in air. Prior to pressing, the inner surfaces of the mold were subjected to thorough mechanical polishing, chemical treatment and cleaning. When pressing the pressure was increased at a rate of 1000 kg/s. The maximum pressure was 12,000 kg/cm^2 (1.2 GPa). The dimensions of the cylindrical samples were: diameter 1 cm, height 0.8...1.4 cm. The characteristics of the samples are given in table 1.

The samples were placed in a corundum crucible and sintered in an air oven at 1,150 °C for 7 hours. After removing the sintered samples, as shown in Fig. 4, compression cracks were found on samples 3, 4 and 5.

Table 1

Compaction of samples of oxide mixtures

№ sample	Weight, g	Pressure, GPa	Notes
1	5	1.2	Half of the sample crumbled when removed from the mold
2	5	0.5	Low strength
3	3	1	There are compression cracks
4	3	1	There are compression cracks
5	3	1	There are compression cracks
6	1.9	1.2	–



a



b



c

**Fig. 4. Appearance of samples after sintering:
a – sample 4; *b* – sample 5; *c* – sample 6**

Sciagrams analysis of the samples showed the presence of phases of the initial oxides and pyrochlorine phase $\text{Y}_2\text{Ti}_2\text{O}_7$. Quantitative phase analysis and calculation



of structural parameters of the samples was performed by the Rietveld method.

The radiographs of the samples are identical within the statistical error (Fig. 5). The amount of pyrochlorine phase is greatest in samples 1 and 6 and is about 20 wt.%.

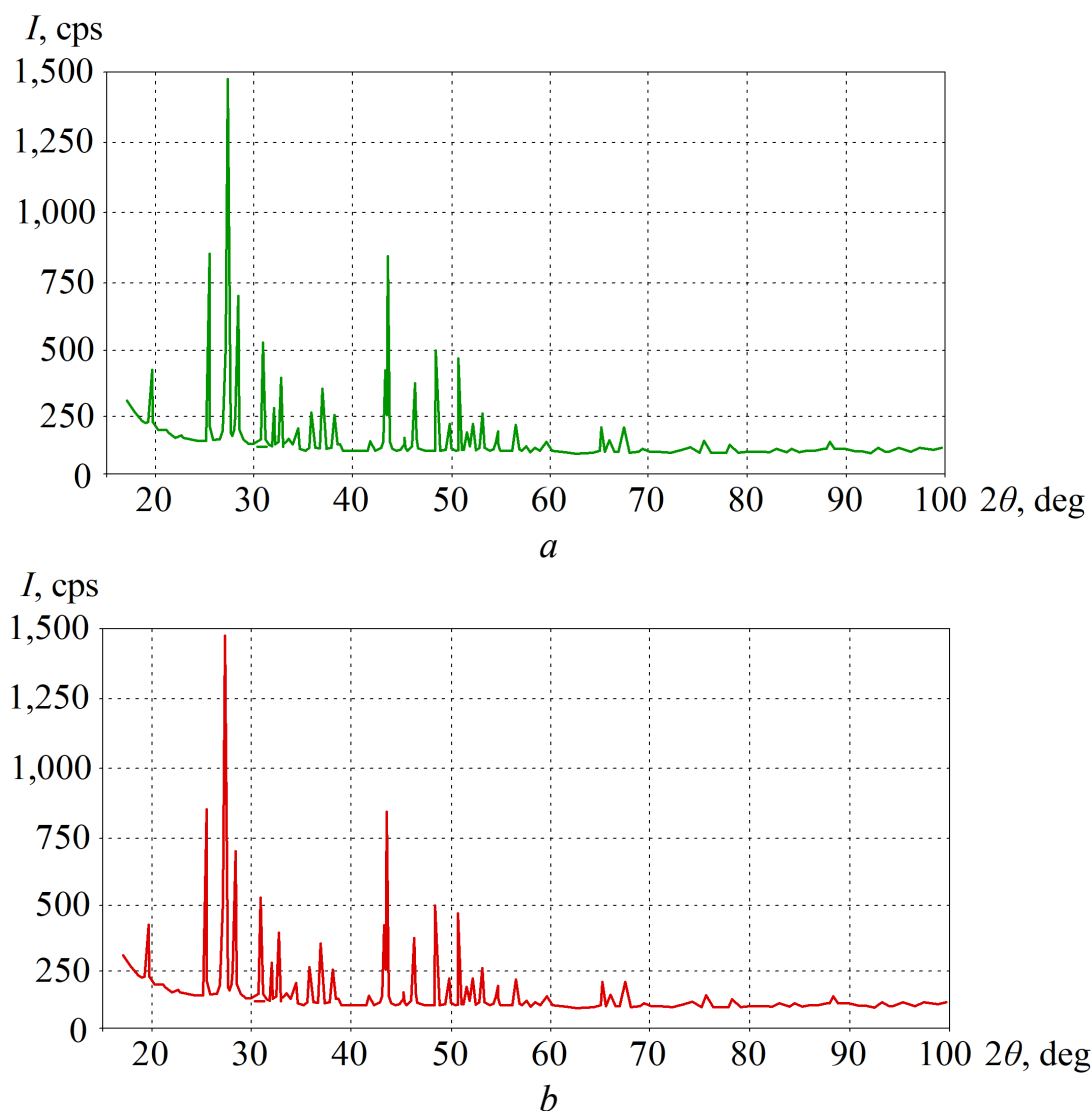


Fig. 5. Sciagrams of samples: *a* – 1 (top); *b* – 6 (lower)

Studies allow us to conclude on the acceptability of the tested technology for the formation of the pyrochlorine phase $\text{Y}_2\text{Ti}_2\text{O}_7$ from a mixture of oxides of yttrium and titanium. To increase the content of the pyrochlorine phase $\text{Y}_2\text{Ti}_2\text{O}_7$ it is necessary to increase the duration of sintering. After additional annealing at 1,150 °C for 10 hours (total annealing duration of 17 hours) according to sciagram data, the sample became almost single-phase. The main phase is yttrium dithitanate $\text{Y}_2\text{Ti}_2\text{O}_7$ (with a weight content of more than 90% in the sample and a lattice parameter of 10.091 Å).

In addition to the pyrochlorine phase, traces of the original oxides of yttrium and titanium were also detected in the sample. The content of yttrium oxide is about 0.5 wt.%, The lattice parameter is equal to 10.597 Å. The rutile content of TiO_2 is close to 2.5 wt.%, The lattice parameters are: $a = 4.591$ Å; $c = 2.959$ Å.

Prolongation of annealing for another 8 hours (up to 25 hours in total) did not lead to significant changes. Although the content of dithitanate in the near-surface



layer increased slightly, traces of the original oxides in the sample are still present (Table 2).

Table 2

Characteristics of sample № 1 after total annealing at 1,150 °C for 25 hours

Phase	$Y_2Ti_2O_7$	Y_2O_3	TiO_2
Content, wt. %	98	0.9	1.1
Lattice parameters, Å	10.092	10.598	$a = 4.593$; $c = 2.959$

In the middle part of the sample, the content of the $Y_2Ti_2O_7$ phase was slightly lower (about 93.4 wt. %), And the initial oxides were slightly higher. This indicates the incompleteness of the synthesis of the pyrochlore phase.

It can be assumed that the removal of large fractions from the source powders and the improvement of pre-compaction will make it possible to reduce the maximum processing temperature to 1,000...1,050 °C. Another promising proposal for further reduction of the synthesis temperature (up to 800 °C) is the use of treatment in a nitrogen-free atmosphere, in an argon environment with certain impurities of oxygen.

Infrared spectra of the studied sample recorded the presence of bands in the range of 650...400 cm^{-1} , which is a characteristic property for oscillations of the Me–O type (metal – oxygen) in cubic structures of the pyrochlore type (Fig. 6).

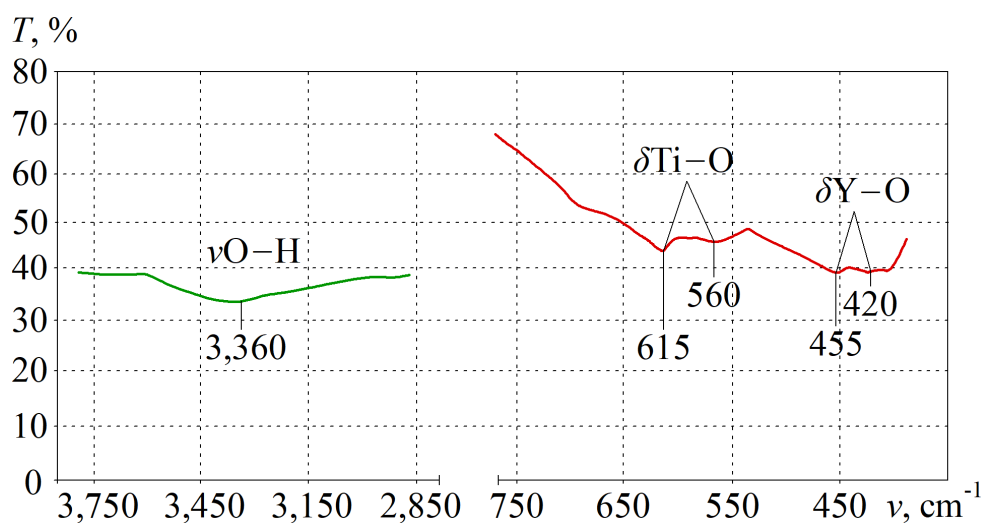


Fig. 6. Infrared absorption spectrum of the sample obtained from yttrium and titanium oxides

Peaks 615 and 560 cm^{-1} are due to Ti–O deformation oscillations in TiO_6 octahedra, and peaks 455 and 420 cm^{-1} are the result of Y–O deformation oscillations. In addition, there is a weak broad band in the spectrum in the region of O–H valence vibrations, which indicates the presence of a small number of hydroxyl groups in the sample structure. The general conclusion of the analysis of the IR spectrum is the statement that the predominant component of the sample material is the phase $Y_2Ti_2O_7$ with a structure of the pyrochlore type.

Conclusion and findings.

Based on the analysis of known literature data and the results of previous studies, technological process schemes for experimental verification of acceptability



and adaptation to existing equipment for materials of the Y–Ti–O system with pyrochlor structure are proposed, namely: for obtaining pure oxides of individual elements. thermal decomposition of salts; for the synthesis of multi-element oxide compounds – the technology of high-temperature synthesis and sintering. Using modernized and optimized technological equipment for high-temperature annealing and compaction of oxide nanopowder compositions, ceramic samples containing pyrochlore phase were obtained.

It is determined that it is possible to realize the synthesis of compounds with the structure of pyrochlor in the treatment with a temperature of 1,150 °C, while increasing the duration of such treatment leads to an increase in the proportion of pyrochlorine phase in the samples. It can be assumed that the removal of large fractions from the source powders and the improvement of pre-compaction will make it possible to reduce the maximum processing temperature to 1,000...1,050 °C.

A promising way to further reduce the synthesis temperature (up to 800 °C) may be the use of treatment in a nitrogen-free atmosphere, in an argon environment with certain oxygen impurities.

References

1. Shi W.-Q., Yuan L.-Y., Li Z.-J., Lan J.-H., Zhao Y.-L., Chai Z.-F. Nanomaterials and nanotechnologies in nuclear energy chemistry. *Radiochimica Acta*. 2014. Vol. 100, Issue 8–9. P. 727–736. DOI: 10.1524/ract.2012.1961.
2. Gevorkyan E. S., Nerubatskyi V. P., Gutsalenko Yu. H., Morozova O. M. Some features of ceramic foam filters energy efficient technologies development. *Modern engineering and innovative technologies*. 2020. Issue 14. Part 1. P. 46–60. DOI: 10.30890/2567-5273.2020-14-01-014.
3. Gevorkyan E. S., Nerubatskyi V. P., Chyshkala V. O., Morozova O. M. Aluminum oxide nanopowders sintering at hot pressing using direct current. *Modern scientific researches*. 2020. Issue 14. Part 1. P. 12–18. DOI: 10.30889/2523-4692.2020-14-01-002.
4. Melnikov P., Nascimento V. A., Consolo L. Z. Mechanism of thermal decomposition of yttrium nitrate hexahydrate, $Y(NO_3)_3 \cdot 6H_2O$ and modeling of intermediate oxynitrates. *J. Therm Anal Calorim*. 2013. Vol. 111. P. 115–119. DOI: 10.1007/s10973-012-2236-3.
5. Tiep N. V., Khiem L. H., Sohatsky A. S., Skuratov V. A., Van Vuuren A. J., O'Connell J. H., Zdorovets M. TEM Study of ODS Alloy Doped with Helium Ions and Re-irradiated with Swift Xe Ions. *Communications in Physics*. 2019. Vol. 29. 3SI. DOI: 10.15625/0868-3166/29/3SI/14286.
6. Gevorkyan E., Nerubatskyi V., Gutsalenko Yu., Melnik O., Voloshyna L. Examination of patterns in obtaining porous structures from submicron aluminum oxide powder and its mixtures. *Eastern-European Journal of Enterprise Technologies*. 2020. Vol. 6, No. 6 (108). P. 41–49. DOI: 10.15587/1729-4061.2020.216733.
7. Азаренков Н. А., Соболев О. В., Береснев В. М., Погребняк А. Д., Литовченко С. В., Иванов О. Н. Материаловедение неравновесного состояния модифицированной поверхности. *Сумской государственный университет*.



2013. 683 с.

8. Азаренков М. О., Неклюдов І. М., Воеводін В. М. та ін. Наноматеріали і нанотехнології: навчальний посібник. Харківський національний університет імені В.Н. Каразіна. 2014. 323 с.

9. Gevorkyan E. S., Rucki M., Kagramanyan A. A., Nerubatskiy V. P. Composite material for instrumental applications based on micro powder Al_2O_3 with additives nano-powder SiC. *International Journal of Refractory Metals and Hard Materials*. 2019. Vol. 82. P. 336–339. DOI: 10.1016/j.ijrmhm.2019.05.010.

10. Mandal B. P., Tyagi A. K. Preparation and high temperature-XRD studies on a pyrochlore series with the general composition $\text{Gd}_{2-x}\text{Nd}_x\text{Zr}_2\text{O}_7$. *J. of Alloys and Compounds*. 2007. Vol. 437. Issue 1–2. P. 260–263.

11. Kunes J., Pickett W. E. KOs_2O_6 : superconducting rattler. *Phys B: Cond.Matter*. 2006. P. 378–380.

12. Yoshimura K., Sakaia H., Ohno H., Kambe S., Walstedt R. E. Physical properties of new superconductor $\text{Cd}_2\text{Re}_2\text{O}_7$ with pyrochlore-type structure. *Physica B: Physics of Condensed Matter*. 2003. Vol. 329. P. 1319–1320.

13. Mandal B. P., Deshpande S. K., Tyagi A. K. Ionic conductivity enhancement in $\text{Gd}_2\text{Zr}_2\text{O}_7$ pyrochlore by Nd doping. *J. Mater. Res.* 2008. Vol. 23. P. 911–916.

14. Mandal B. P., Dutta A., Deshpande S. K., Basu R. N., Tyagi A. K. Nanocrystalline $\text{Nd}_{2-y}\text{Gd}_y\text{Zr}_2\text{O}_7$ pyrochlore: Facile synthesis and electrical characterization. *J. Mater. Res.* 2009. Vol. 24, Issu 9. P. 2855–2862.

15. Garg N., Pandey K. K., Murli C., Shanavas K. V., Mandal B. P., Tyagi A. K., Sharma S. M. Decomposition of lanthanum hafnate at high pressures. *Phys. Rev. B*. 2008. Vol. 77, Issue 21. P. 214105.

16. Sickafus K. E., Minervini L., Grimes R. W., Valdez J. A., Ishimaru M., Li F., McClellan K. J., Hartmann T. Radiation Tolerance of Complex Oxides. *Science*. 2000. Vol. 289, Issue 5480. P. 748–751.

17. Skuratov V. A., Sohatsky A. S., O'Connell J. H., Kornieieva K., Nikitina A. A., Neethling J. H., Ageev V. S. Swift heavy ion tracks in $\text{Y}_2\text{Ti}_2\text{O}_7$ nanoparticles in EP450 ODS steel. *Journal of Nuclear Materials*. 2015. Vol. 456. P. 111–114.

18. Rietveld H. M. A profile refinement method for nuclear and magnetic structures. *Journal of Applied Crystallography*. 1969. Vol. 2. P. 65–71.

19. Melnikov P., Nascimento V. A., Consolo L. Z., Silva A. F. Mechanism of thermal decomposition of yttrium nitrate hexahydrate, $\text{Y}(\text{NO}_3)_3 \cdot 6\text{H}_2\text{O}$ and modeling of intermediate oxynitrates. *Journal of Thermal Analysis and Calorimetry*. 2013. Vol. 111, Issue 1. P. 115–119.

20. Геворкян Э. С., Нерубацкий В. П., Мельник О. М. Горячее прессование нанопорошков состава ZrO_2 -5% Y_2O_3 . *Збірник наукових праць Української державної академії залізничного транспорту*. 2010. Вип. 119. С. 106–110.

21. Нерубацький В. П. Моделювання процесу гарячого пресування при спіканні тугоплавких нанопорошкових з'єднань. *Матеріали XVII міжнародної науково-практичної конференції «Інформаційні технології: наука, техніка, технологія, освіта, здоров'я» (Харків, 20–22 травня 2009 р.)*. Харків: НТУ «ХПІ», 2009. Ч. 1. С. 362.